

# The shallow-decay phase in both the optical and X-ray afterglows of *Swift* GRB 090529A: energy injection into a wind-type medium?

L. P. Xin,<sup>1\*</sup> A. Pozanenko,<sup>2</sup> D. A. Kann,<sup>3</sup> D. Xu,<sup>4</sup> J. Gorosabel,<sup>5</sup> G. Leloudas,<sup>4</sup>  
J. Y. Wei,<sup>1</sup> M. Andreev,<sup>6,7</sup> S. F. Qin,<sup>1</sup> M. Ibrahimov,<sup>8</sup> X. H. Han,<sup>1</sup>  
A. de Ugarte Postigo,<sup>4</sup> Y. L. Qiu,<sup>1</sup> J. S. Deng,<sup>1</sup> A. Volnova,<sup>9</sup> P. Jakobsson,<sup>10</sup>  
A. J. Castro-Tirado,<sup>5</sup> F. Aceituno,<sup>11</sup> J. P. U. Fynbo,<sup>4</sup> J. Wang,<sup>1</sup> R. Sanchez-Ramirez,<sup>5</sup>  
V. Kouprianov,<sup>12</sup> W. K. Zheng,<sup>13</sup> J. C. Tello<sup>5</sup> and C. Wu<sup>1</sup>

<sup>1</sup>National Astronomical Observatories, Chinese Academy of Sciences, Beijing 100012, China

<sup>2</sup>Space Research Institute (IKI), 8432 Profsoyuznaya str., Moscow, 117997, Russia

<sup>3</sup>Thüringer Landessternwarte Tautenburg, Sternwarte 5, 07778, Tautenburg, Germany

<sup>4</sup>Dark Cosmology Centre, Niels Bohr Institute, University of Copenhagen, Juliane Maries Vej 30, 2100 Copenhagen, Denmark

<sup>5</sup>Instituto de Astrofísica de Andalucía (IAA-CSIC), PO Box 3004, 18080 Granada, Spain

<sup>6</sup>Terskol Branch of Institute of Astronomy of RAS, Kabardino-Balkaria Republic 361605, Russian Federation

<sup>7</sup>International Centre of Astronomical and Medico-Ecological Research of NASU, 27 Akademika Zabolotnogo str., 03680, Kyiv, Ukraine

<sup>8</sup>Ulugh Beg Astronomical Institute, Tashkent 700052, Uzbekistan

<sup>9</sup>Sternberg Astronomical Institute, Moscow State University, Universitetsky pr., 13, Moscow 119992, Russia

<sup>10</sup>Centre for Astrophysics and Cosmology, Science Institute, University of Iceland, Dunhagi 5, IS-107 Reykjavik, Iceland

<sup>11</sup>Observatorio de Sierra Nevada, Instituto de Astrofísica de Andalucía (IAA-CSIC), PO Box 3004, 18080 Granada, Spain

<sup>12</sup>Main Astronomical Observatory of RAS, Pulkovo, St Petersburg 196140, Russia

<sup>13</sup>Department of Physics, University of Michigan, Ann Arbor, MI 48109, USA

Accepted 2012 February 1. Received 2012 January 31; in original form 2011 October 8

## ABSTRACT

The energy injection model is the usual choice for interpreting the shallow-decay phase in *Swift* gamma-ray burst (GRB) X-ray afterglows. However, very few GRBs have simultaneous signatures of energy injection in their optical and X-ray afterglows. Here, we report on the optical observations of GRB 090529A from 2000 s to  $\sim 10^6$  s after the burst, in which an achromatic decay is seen at both wavelengths. The optical light curve shows a decay from 0.37 to 0.99, with a break at  $\sim 10^5$  s. In the same time interval, the decay indices of the X-ray light curve changed from 0.04 to 1.2. Comparing these values with the closure relations, the segment after  $3 \times 10^4$  s is consistent with the prediction of the forward shock in an interstellar medium without any energy injection. The shallow-decay phase between 2000 and  $3 \times 10^4$  s could be a result of the external shock in a wind-type medium with an energy injection under the condition of  $\nu_o < \nu_c < \nu_x$ . However, the constraint of the spectral region is not consistent with the multiband observations. For this shallow-decay phase, other models are also possible, such as energy injection with evolving microphysical parameters, a jet viewed off-axis, etc.

**Key words:** gamma-ray burst: general – gamma-ray burst: individual: GRB 090529A.

## 1 INTRODUCTION

Gamma-ray bursts (GRBs) are considered to be produced by the merger of binary compact stars (Type I GRBs), or by the death of massive stars (Type II GRBs; e.g. Paczyński 1998; Zhang et al. 2009), with a relativistic fireball shell (ejecta) expanding into a uniform interstellar medium (ISM), or the pre-burst stellar wind

of the progenitor star with a density distribution of  $\rho \propto R^{-2}$  (e.g. Chevalier & Li 1999; Dai & Lu 1998a). The standard fireball model (Sari, Piran & Narayan 1998) was capable of interpreting most observations before *Swift*. Since *Swift* was launched in 2004 (Gehrels et al. 2004), our understanding of GRB physics has been revolutionized by many unexpected discoveries from space- and ground-based observations. Almost half of the *Swift* GRBs show canonical light curves in their X-ray afterglows, and the origin of shallow-decay behaviour is much debated (e.g. Granot 2006; Nousek et al. 2006; Zhang et al. 2006; Liang, Zhang & Zhang 2007; Evans et al. 2009).

\*E-mail: xlp@nao.cas.cn

Several models have been proposed to interpret this behaviour, such as prior emission (Yamazaki 2009; Liang et al. 2010), off-axis jet viewing (Granot et al. 2002; Eichler & Granot 2006), X-ray dust scattering (Shao & Dai 2007), evolving microphysical parameters (Granot, Königl & Piran 2006; Panaitescu et al. 2006) and energy injection (Dai & Lu 1998b,c; Sari & Mészáros 2000; Nousek et al. 2006; Zhang et al. 2006).

In the literature, the signature of energy injection has been reported for a few GRB afterglows. For example, GRB 050408 (de Ugarte Postigo et al. 2007), whose multiband light curve shows a re-brightening phase at 2.9 d after the burst achronically, is considered to be a likely off-axis event with an energy injection. This is also thought to have occurred in both the X-ray and optical afterglows of GRB 071010A (Covino et al. 2008), whose sharp re-brightening at 0.6 d after the burst is considered as a discrete energy injection. The plateau phases in both the X-ray and optical afterglows of GRB 061121 are consistent with an injection of energy (Page et al. 2007), but the transition from plateau to the later phase is only visible in X-ray afterglows. A long-duration shallow-decay phase in both the X-ray and optical afterglows is also evident in the long-duration GRB 060729 ( $T_{90} = 105$  s; Grupe et al. 2007), which could be well explained via a long-term energy injection. The transition breaks between the shallow-decay and normal-decay phases lie at about 60 and about 50 ks for the X-ray and optical afterglows, respectively. There are many further examples of GRBs that feature strong energy injections in the optical, but that are hardly or not at all visible in X-rays (usually because of sparse coverage): for example, GRB 021004 (e.g. de Ugarte Postigo et al. 2005), GRB 030329 (e.g. Lipkin et al. 2004), GRB 060206 (Monfardini et al. 2006; Woźniak et al. 2006), GRB 060526 (Dai et al. 2007; Thöne et al. 2010), GRB 070125 (Utdike et al. 2008) and GRB 090926A (Rau et al. 2010; Cenko et al. 2011).

Like GRB 060729, GRB 090529A is another good example where both the optical and X-ray afterglows have a long-term energy injection before the phase of normal achromatic decay. Thus, it is a good candidate for us to use in a detailed study of this topic. Both the X-ray and optical afterglows show shallow-decay segments within a similar time range, followed by a steeper, almost achromatic, decay. This behaviour can be interpreted as an energy injection via a refreshed shock or late-time central engine activity.

In this paper, we report on our observations of the optical afterglow for GRB 090529A using several ground-based optical telescopes. The optical and X-ray afterglow data are used to explore the nature of this event. We report on our observations in Section 2. We present a joint optical and X-ray data analysis and discussion in Section 3, and we give the energy budget in Section 4. We provide our summary and conclusions in Section 5. The notation  $f_\nu \propto t^{-\alpha} \nu^{-\beta}$  is used throughout the paper, where  $f_\nu$  is the spectral flux density at the frequency  $\nu$ .

## 2 OBSERVATIONS AND DATA REDUCTION

GRB 090529A was detected by the Burst Alert Telescope (BAT) onboard *Swift* (Sakamoto et al. 2009a) at 14:12:35 UT on 2009 May 29 (trigger 353540) during a pre-planned slew. Because *Swift* did not observe the start of the burst, its  $T_{90}$  duration can only be given as a lower limit. However, it is still longer than 100 s in the 15–350 keV band (Markwardt et al. 2009), and therefore it belongs to a long-duration class of bursts (Kouveliotou et al. 1993). It is interesting that no other missions detected this burst. Even the Spectrometer for *INTEGRAL* (SPI) Anticoincidence Shield (ACS), which could have detected the burst, has no rate increase in the data around the trigger

time for GRB 090529. Most probably, the burst was too soft to be detected by the SPI ACS. The significant short spike, with a duration of 0.1 s, occurred 20 s before the trigger time.<sup>1</sup> However, there is no clear relationship between the spike and GRB 090529. The *Swift* X-ray Telescope (XRT) began to observe the burst 197.1 s after the burst, and it found a counterpart. Meanwhile, no new source was found in the first white finding chart of the *Swift* Ultraviolet/Optical Telescope (UVOT) instrument, but a new source was detected in the second white image at 883 s after the burst trigger (Sakamoto et al. 2009a). The optical afterglow was observed by several ground-based telescopes, and its spectroscopic redshift of  $z = 2.63$  was determined by the European Southern Observatory (ESO) Very Large Telescope (Malesani et al. 2009). The time-integrated gamma-ray spectrum is fitted well by a single power law with a photon index of  $2.0 \pm 0.3$  (Markwardt et al. 2009). The fluence in the 15–150 keV band is  $6.8 \pm 1.7 \times 10^{-7}$  erg cm<sup>-2</sup>. The isotropic energy  $E_{\text{iso}}$  is estimated to be about  $7 \times 10^{52}$  erg. With the relation between the photon index  $\Gamma$  and the observational peak energy  $E_{\text{peak,o}}$  obtained by simulations (Sakamoto et al. 2009c), the peak energy  $E_{\text{peak,o}}$  in the observational frame can be inferred as  $40 \pm 23$  keV. Therefore, this burst would be consistent with the Amati relationship (Amati et al. 2002) like most long-duration GRBs.

### 2.1 *Swift* XRT X-ray afterglow

The *Swift* XRT light curve and spectrum are extracted from the UK *Swift* Science Data Centre at the University of Leicester (Evans et al. 2009).<sup>2</sup> We also fit the X-ray spectrum with the XSPEC package. The time-integrated X-ray spectrum from all the photon counting (PC) mode data after 3 ks– $3 \times 10^4$  s is well fitted by an absorbed power-law model, with a photon power-law index  $\Gamma = 1.6^{+0.54}_{-0.37}$ . No significant host  $N_{\text{H}}$  excess over the Galactic value is detected. The time-integrated X-ray spectrum  $3 \times 10^4$  s after the trigger can be fitted with a power-law model with a photon power-law index of  $\Gamma = 2.53^{+1.45}_{-0.96}$ . The two  $\Gamma$  values agree with each other within errors as a result of large uncertainties, so there is no significant evidence for spectral evolution.

### 2.2 Optical afterglow

The 0.8-m Tsinghua University–National Astronomical Observatories Telescope (TNT) is located at Xinglong Observatory in China. GRB 090529A was observed by the TNT, starting from May 29, 14:36:54 UT, 24.3 min after the burst. A series of clear ( $C_R$ ) and  $R$ -band images was obtained. This led to the identification of the optical counterpart.

The Maidanak AZT-22 (1.5-m) telescope is located at Maidanak Observatory, in the south-east of the Republic of Uzbekistan. It observed the optical afterglow of GRB 090529A several times from 0.15 d to 0.2 d, and a series of images in the  $R$  band was obtained. The optical counterpart was detected in all the single images.

The 1.34-m Schmidt telescope of the Thüringer Landessternwarte Tautenburg (TLS) in Germany, began to observe the optical afterglow at 6.6 h after the burst. Six dithered  $I_C$ -band images, with an exposure time of 300 s for each single image, and six images in the  $R_C$  band, with an exposure time of 600 s each, were obtained.

The optical afterglow was observed by the Zeiss-600 telescope (Zeiss-600) of Mt Terskol Observatory in the  $R$ -band filter on May

<sup>1</sup> <http://www.isdc.unige.ch/integral/science/grb>

<sup>2</sup> [http://www.swift.ac.uk/xrt\\_products/](http://www.swift.ac.uk/xrt_products/)

29 between 19:40 and 20:20 UT. The optical counterpart of this burst can be detected in the combined image with a total time exposure of 2400 s.

The optical afterglow was also observed by the MTM-500 telescope of the Kislovodsk solar station of the Pulkovo Observatory in the *R* band for several series on May 29 between 19:58 and 22:20 UT. The optical counterpart was detected in combined images.

The 1.5-m Observatorio de Sierra Nevada (OSN) telescope carried out *R*-band observations of GRB 090529A on May between 29.87 and 29.93 UT, 0.27–0.33 d after the GRB. The optical afterglow was detected in the combined image with a total exposure time of 4800 s.

The Nordic Optical Telescope (NOT), carried out multiple follow-up observations of GRB 090529A, starting 1.29 d after the burst and up to 6 d after the trigger. Several *R*-band images were obtained. Each of these images has an exposure time of 600 s. The optical afterglow is well detected in these images.

Data reduction was carried out following standard routines in the IRAF<sup>3</sup> package, including bias and flat-field corrections. Point spread function (PSF) photometry was applied using the DAOPHOT task in the IRAF package to obtain the instrumental magnitudes. During the reduction, some frames were combined in order to increase the signal-to-noise ratio (S/N). In the calibration and analysis, the TNT  $C_R$  band was treated as the *R* band, because they are similar to each other within uncertainties of 0.07 mag (Xin et al. 2010). TLS images were reduced in a standard fashion and analysed under MIDAS<sup>4</sup> using seeing-matched aperture photometry. Absolute calibration was performed using the Sloan Digital Sky Survey (SDSS; Adelman-McCarthy et al. 2008), with a conversion of the SDSS to the Johnson–Cousins system (Lupton et al. 2005).<sup>5</sup> The optical data of GRB 090529A observed by TNT, Maidanak, TLS, Z-600, OSN and NOT are reported in Table 1. For completeness, the *R*-band data from GCN Circular 9485 (Balman et al. 2009) presented here are recalibrated with SDSS reference stars.

### 3 ANALYSIS AND DISCUSSION

#### 3.1 Light curves

We correct the extinction of our Galaxy [ $E(B - V) = 0.023$ ; Schlegel, Finkbeiner & Davis 1998], and then we plot the optical *R*-band light curve in Fig. 1. First, we fit the *R*-band light curve 1000 s after the burst with a simple single power law  $f \sim t^{-\alpha_{\text{pl}}}$ . The temporal slope  $\alpha_{\text{pl}}$  is  $0.5 \pm 0.01$ . The reduced  $\chi^2$  is 2.47, with 32 degrees of freedom. We then fit the same data with a smoothly broken power-law model, yielding two decaying slopes of  $0.37 \pm 0.03$  and  $0.99 \pm 0.12$ , respectively, with a broken time of  $\sim 9.5 \times 10^4$  s. The reduced  $\chi^2$  is 1.08, with 30 degrees of freedom, as shown in equation (1). Thus, it is better to use the smooth broken power-law model rather than the single power-law model to fit the optical light curve:

$$F = F_0 \left[ \left( \frac{t}{t_b} \right)^{\omega\alpha_1} + \left( \frac{t}{t_b} \right)^{\omega\alpha_2} \right]^{-1/\omega}. \quad (1)$$

<sup>3</sup> IRAF is distributed by the National Optical Astronomy Observatory, which is operated by Association of Universities for Research in Astronomy, Inc., under cooperative agreement with National Science Foundation.

<sup>4</sup> <http://www.eso.org/sci/software/esomidas/>

<sup>5</sup> <http://www.sdss.org/dr6/algorithms/sdssUBVRITransform.html#Lupton2005>

The *Swift* UVOT white-band data (Sakamoto et al. 2009b) are also plotted in Fig. 1. In order to compare *R*-band data with *Swift* UVOT data, we shift the UVOT white-band data to the flux level of our Johnson *R*-band data, 1000 s after the burst. We find that the *R*-band and UVOT light curves trace each other well after 1000 s. Assuming that they also trace each other well before 1000 s, we can infer the behaviour of the *R*-band light curve before 1000 s from the properties of the UVOT white-band light curve.

The UVOT data at the early phase show an upper limit at the first observation, and a positive detection at the second data point. The latter is apparently brighter than the first observation. Other later data became fainter than the second data point for about 0.5 mag, and they decayed continuously, with a shallow decay slope of  $\sim 0.3$ . Considering only the second and third data points of the UVOT observations, the decay index between these two measurements is about  $1.24 \pm 0.3$ , which is not likely to be the emission from reverse shock, as for GRB 990123 (Akerlof et al. 1999). The existence of the brightest flux of the second white data point implies that either the onset of the early afterglow or an early optical flare has taken place before the shallow-decay phase. However, because of the sparse data, the origin of the early UVOT white observations is not clear.

The *Swift* X-ray light curve is also plotted and fitted in Fig. 1. The X-ray afterglow shows a *Swift* canonical X-ray light curve with a steep decay during the first observations up to about 3000 s. Then, this turns into the shallow-decay phase with a decay index of  $0.04 \pm 0.20$ , which is followed by a normal decay with a decay slope of  $1.17 \pm 0.17$ . All these fit parameters are summarized in Table 2.

We note that GRB 090529A was triggered in image mode, and that it was already ongoing when it came into the field of view during a pre-planned slew. This means that there was emission prior to the trigger time for at least 50 s. Therefore,  $T_0$  might be shifted to an earlier time by at least 50 s relative to the trigger time. Consequently, this affects the decay slopes of the afterglow emission. However, we have checked that even we shift  $T_0$  to 50 s before the trigger time, our fitting results are not greatly affected, because the start time of the shallow-decay phase is much later, about  $\sim 10^3$  s after the burst.

#### 3.2 Normal-decay phase

In the normal-decay phase of the X-ray afterglow, the emission process is usually in the slow-cooling regime. For GRB 090529A, the temporal decay index  $\alpha_x$  and spectral index  $\beta_x$  are  $1.17 \pm 0.17$  and  $1.53^{+1.45}_{-0.96}$ , respectively. These values are roughly consistent with the predictions of the external forward-shock model for the spectral regime  $\nu_x > \max(\nu_c, \nu_m)$  (Liang et al. 2008). Additionally, the X-ray light curve is steeper than the optical light curve by  $\delta\alpha \sim 0.2$ . This indicates that the external medium is ISM and that  $\nu_o < \nu_c < \nu_x$  during the power-law decay phase. In this regime, the electron energy distribution index  $p$  can be estimated using the relation  $p = (4\alpha_x + 2)/3 \sim 2.2$ . This is consistent with the typical value ( $p \sim 2.36$ ) for the electron energy distribution index in the GRB model (Curran et al. 2010). However, because of the larger uncertainties of the decay slopes, the difference between the X-ray and optical afterglows of  $\delta\alpha \sim 0$  cannot be excluded.

#### 3.3 Shallow-decay phase

##### 3.3.1 Spectral index

In order to investigate the origin of the shallow-decay segments in both the optical and X-ray afterglows, the spectral index from

**Table 1.** Optical afterglow photometry log of GRB 090529A. The reference time  $T_0$  is the *Swift* BAT burst trigger time of 14:12:35 UT. The data have not been corrected for the Galactic extinction [ $E(B - V) = 0.021$ ; Schlegel et al. 1998]. The first column of this table is the mean time.

$T - T_0$ (min)	Exposure (s)	Filter	Magnitude	Mag_Err	Telescope
25.825	160	$C_R$	19.84	0.14	TNT
29.627	240	$C_R$	19.92	0.12	TNT
37.230	600	$R$	20.05	0.12	TNT
47.843	600	$R$	19.98	0.11	TNT
58.427	600	$R$	19.99	0.11	TNT
69.025	600	$R$	20.18	0.11	TNT
79.610	600	$R$	20.47	0.13	TNT
100.368	1800	$R$	20.22	0.10	TNT
131.198	1800	$R$	20.43	0.11	TNT
162.030	1800	$R$	20.64	0.14	TNT
218.548	4800	$R$	20.66	0.15	TNT
223.330	300	$R$	20.73	0.07	Maidanak
229.795	300	$R$	20.70	0.05	Maidanak
235.987	300	$R$	20.65	0.05	Maidanak
242.597	300	$R$	20.75	0.06	Maidanak
248.083	300	$R$	20.59	0.05	Maidanak
253.583	300	$R$	20.80	0.06	Maidanak
259.070	300	$R$	20.72	0.07	Maidanak
265.420	300	$R$	20.76	0.06	Maidanak
270.907	300	$R$	20.75	0.07	Maidanak
276.380	300	$R$	20.80	0.06	Maidanak
281.880	300	$R$	20.72	0.06	Maidanak
287.367	300	$R$	20.76	0.06	Maidanak
294.020	300	$R$	20.73	0.06	Maidanak
299.505	300	$R$	20.76	0.06	Maidanak
347.415	2400	$R$	20.94	0.23	Zeiss-600
405.648	3600	$R$	20.70	0.25	MTM-500 <sup>a</sup>
478.656	3600	$R$	21.30	0.40	MTM-500 <sup>a</sup>
414.535	1800	$I_C$	20.27	0.09	TLS
432.000	4800	$R$	21.01	0.05	OSN
438.722	600	$R_C$	21.11	0.13	TLS
449.555	600	$R_C$	21.13	0.13	TLS
460.372	600	$R_C$	21.23	0.43	TLS
596.160	900	$R$	20.90	0.20	GCN 9485 <sup>b</sup>
663.462	1800	$R_C$	21.00	0.11	TLS
1874.800	600	$R$	21.81	0.05	NOT
1885.750	600	$R$	21.77	0.05	NOT
1896.550	600	$R$	21.88	0.05	NOT
4774.000	1800	$R$	22.79	0.12	NOT
9145.420	1800	$R$	23.06	0.20	NOT

<sup>a</sup> The photometry supersedes the result reported in Volnova et al. (2009).

<sup>b</sup> These data are derived from the literature (Balman et al. 2009). We have recalibrated the brightness with SDSS reference stars.

optical to X-ray would be helpful. To obtain the intrinsic optical flux, the extinction caused by our Galaxy in the direction of the bursts is corrected for, which is  $E(B - V) = 0.021$  (Schlegel et al. 1998), corresponding to  $A_R = 0.055$  mag and  $A_I = 0.040$ . The extinction from the GRB host is not considered here. The extinction-corrected magnitudes are converted into flux densities.

For the  $R$ -band data, we interpolated the data with the best-fitting data during this phase. For the  $I$ -band data, we extrapolated the data with the fitting result of the  $R$ -band light curve, assuming that the decay indices of the light curves in both frequencies are the same in the shallow phase. The time we calculate for the optical bands is about 15 ks after the burst. Fig. 2 shows the X-ray spectrum during the shallow-decay phase with its power-law index and its errors as well as the  $R$ -band flux density. It is evident that the optical flux is located in the extrapolation of the X-ray spectral index within  $1\sigma$  errors. The optical ( $R$ -band) to X-ray spectral index  $\beta_{\text{OX}}$  is very

similar to the observed X-ray spectral index of  $\sim 0.6$ . This suggests that the extinction from the host galaxy could be negligible.

### 3.3.2 Classical external-shock model?

According to the classical external-shock model (Mészáros, Rees & Wijers 1998; Sari et al. 1998; Sari, Piran & Halpern 1999; Chevalier & Li 2000; Dai & Cheng 2001; Zhang et al. 2006), the optical and X-ray afterglows have closure relations under several conditions. We notice that the optical light curve decays more steeply than the X-ray light curve by about  $\delta\alpha \sim 0.37$  at the shallow-decay phase. This is consistent with the condition of a wind-type medium in the spectral region of  $\nu_0 < \nu_c < \nu_x$ . In detail, assuming that the medium has a density distribution of  $\rho \propto R^{-s}$ , in the condition of no energy injection, the decay indices of the optical and X-ray emission would

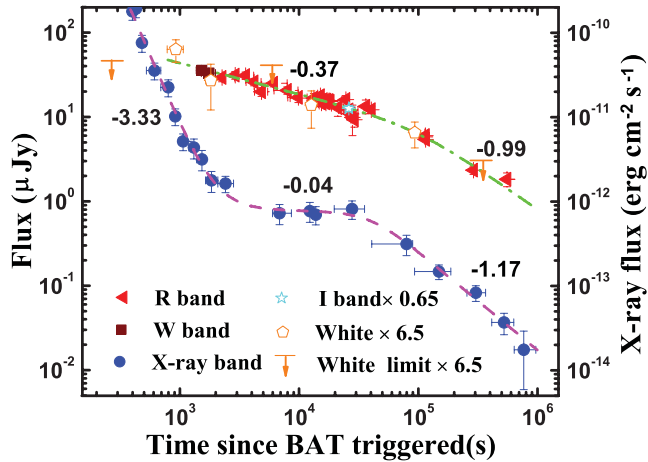


**Figure 1.** Optical and X-ray light curves of GRB 090529A. The optical light curve can be fitted with a smoothly broken power-law model with an index transition from  $\alpha_{O1} = 0.37 \pm 0.03$  to  $\alpha_{O2} = 0.99 \pm 0.12$ . The X-rays show a canonical light curve with an initial steep-decay phase, and then a shallow-decay phase with an index of  $\alpha_{X1} = 0.04 \pm 0.20$ , which is followed by a normal-decay phase with an index of  $\alpha_{X2} = 1.17 \pm 0.17$ . *Swift* UVOT white-band data are also plotted and shifted in flux density for completeness and comparison.

have a relation  $\alpha_o - \alpha_x = -0.25 + s/(8 - 2s)$  (Urata et al. 2007) in the classical external-shock model for the case of  $v_o < v_c < v_x$ . With these parameters ( $\alpha_o \sim 0.37 \pm 0.03$  and  $\alpha_x \sim 0.04 \pm 0.20$ ) of GRB 090529A in this phase, we can infer that the density parameter  $s \sim 2$ . This is consistent with the theoretical prediction of a wind-type medium ( $\rho \propto R^{-2}$ ). Therefore, it seems that the environment of the shallow-decay phase in both X-ray and optical emissions should be a wind-type medium. However, the requirement of the spectral indices between the optical and X-ray emission seems to be inconsistent with the result of Fig. 2. A possible solution for this conflict is that the cooling frequency should be marginally above the optical band. However, as a consequence, the optical spectral index would be about  $\beta_{opt} = 0.1^{+0.54}_{-0.37}$  according to the relation  $\beta_{opt} = \beta_x - 0.5$ . However, this appears to disagree with the  $I_C$ -band data point from the TLS observation.

### 3.3.3 Energy injection?

Considering the shallow-decay indices, continuous energy injection might be occurring (Dai & Lu 1998b; Sari & Mészáros 2000; Nousek et al. 2006; Zhang et al. 2006). Here, new energy is injected into the forward shock and it forms ‘refreshed shocks’, making the temporal decay indices shallower. This new energy can be produced in two ways: (i) by the long-lasting activity of the central engine, with the transformation of the Poynting flux energy into kinetic energy in the external shock (Dai & Lu 1998b); (ii) by a brief and short-duration central engine activity, which ejects shells with a

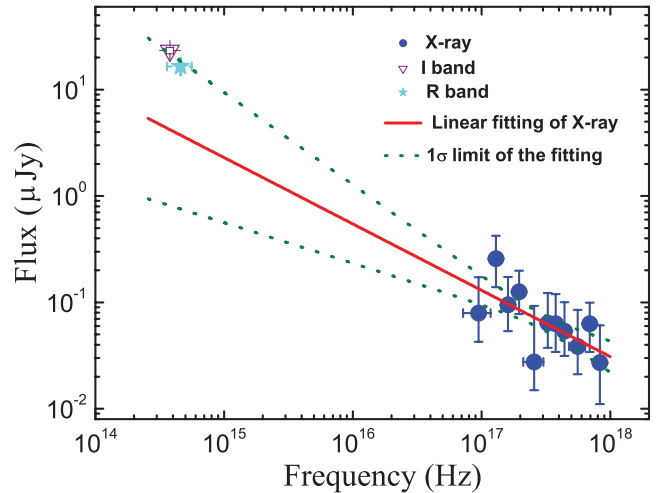


**Figure 2.** Spectrum of the X-ray afterglow for GRB 090529A in the time range 3 ks–30 ks after the burst. The optical data points (*R* and *I* bands) are shown by a star and a triangle, respectively.

range of Lorentz factors, such that slower ejecta catch up with the decelerated shock (Zhang et al. 2006, and references therein).

For the first case of Poynting flux energy injection, the injected luminosity is given by  $L(t) = L_0(t/t_b)^{-q}$  (Zhang et al. 2006). Given the closure relationship for  $\alpha$  and  $\beta$  of afterglows in various GRB models (Zhang et al. 2006), and for the measured values of the X-ray afterglow of GRB 090529A ( $\alpha_x = 0.04 \pm 0.02$  and  $\beta_x = 0.6^{+0.54}_{-0.42}$ ), we estimate that the energy injection index is  $q = 2(\alpha + 1 - \beta)/(2 + \beta) \sim 0.34 \pm 0.45$  for  $v_x > v_c$  in a wind medium and the slowing cooling phase. Because the optical frequency should be located at the spectral region  $v_{opt} < v_c < v_x$ , the closure relation via the energy injection would be  $q = 2(\alpha - \beta)/(1 + \beta)$  for the optical band. In this case, the energy-injection parameter  $q$  would be  $0.5 \pm 0.5$  for the optical indices of  $\alpha_{opt} = 0.37 \pm 0.03$  and  $\beta_{opt} = 0.1^{+0.54}_{-0.37}$ . The two values of  $q$  for both optical and X-ray afterglows are consistent with each other within their uncertainties. This implies that the new-formed energy is injected into the forward shock, making the light curve shallower for both X-ray and optical bands simultaneously.

For the second case of a range of Lorentz factors in the ejecta, which follow the form of  $M(>\gamma) \sim \gamma^{-s}$  ( $s > 1$ ; Zhang et al. 2006), with our measured value of  $q \sim 0.4$  (the average value for the optical and X-ray bands), the Lorentz factor index  $s$  would be about 7 for the wind model (Nousek et al. 2006; Zhang et al. 2006). This result corresponds to the total energy in the fireball decreasing as  $E_{iso} \propto \gamma^{1-s} \sim \gamma^{-6}$ .

It is likely that the simultaneous shallow-decay phase of GRB 090529A in both the X-ray and optical afterglows could be interpreted by energy injection in a wind-type medium by a long-lasting central-engine activity or a range of Lorentz factors in the ejecta. Meanwhile, the normal-decay phase can be explained by the standard forward shock in an ISM. Therefore, it seems that the break from the shallow- to normal-decay phase could be caused by the

**Table 2.** X-ray and optical light curves 3000 s after the burst are fitted with a smoothly broken power-law model.

Interval	$F_0$	$t_b$ (s)	$\alpha_1$	$\alpha_2$	$\omega$ (fixed)	$\chi^2/\text{dof}$
X-ray	$7.396 \pm 2.371^a$	$40\,095 \pm 17\,760$	$0.04 \pm 0.20$	$1.17 \pm 0.17$	3	61/59
Optical	$8.10 \pm 1.27$	$95\,042 \pm 23\,457$	$0.37 \pm 0.03$	$0.99 \pm 0.12$	3	32.48/30

<sup>a</sup>In units of  $\times 10^{-13}$  erg cm $^{-2}$  s $^{-1}$ .

cessation of energy injection. Simultaneously, the external medium would also have a transition from a wind-type to constant-density ISM (e.g. Dai & Lu 2002; Dai & Wu 2003). However, it is unlikely that these two different processes can take place at the same time.

### 3.3.4 Other models

*Evolving microphysical parameters.* Panaitescu et al. (2006) generalized the formulae for the synchrotron-shock model by including the variations of some physical parameters in the blast wave: the energy injection  $E(> \Gamma) \propto \Gamma^{-e}$ , the energy ratio for the magnetic field  $\epsilon_B \propto \Gamma^{-b}$ , the energy ratio for electrons  $\epsilon_i \propto \Gamma^{-i}$  and the ambient medium density  $n(r) \propto r^{-s}$ . As shown in equations (9) and (10) of Panaitescu et al. (2006), the decay indices for the optical and X-ray light curves in the spectral region  $\nu_o < \nu_c < \nu_x$  are derived. A general relationship between  $\alpha_o$  and  $\alpha_x$  can be expressed by (Urata et al. 2007)

$$\alpha_o - \alpha_x = \frac{s}{8-2s} - \frac{1}{4} + \frac{3-s}{e+8-2s} \left[ \left( \frac{s}{8-2s} - \frac{1}{4} \right) e - \frac{3}{4}b \right], \quad (2)$$

which is independent of  $p$  and  $i$  but has some dependence on  $e$  and  $b$ . Assuming  $s = 0$  (ISM case), for GRB 090529A, we obtain  $(e + 3b)/(e + 8) = -0.72 \times 4/3 < 0$ , which requires that at least one of  $e$  or  $b$  is negative, which is an unphysical condition. However, if we assume that  $s = 2$  (wind-type medium), we obtain  $0.72e - 3b = 1.76$ . This means that when new energy is injected into the wind-type medium, not only are the microphysical parameters evolving, but also the energy injection fraction and the energy ratio for the magnetic field should have a relationship ( $0.72e - 3b = 1.76$ ) to meet the case of GRB 090529A.

*Off-axis viewing jet model.* Another explanation for the plateau phase is that the afterglow is observed from viewing angles slightly outside the jet. Depending on the jet structures, dynamics, viewing angle (e.g. Eichler & Granot 2006; Marshall et al. 2011), the light curve can have a long shallow-decay phase at early times or an initial rising phase after the prompt emission. This is generally consistent with the case of GRB 090529A at the early phase, except for the earliest detections of a flare-like or re-brightening-like feature by the UVOT. However, the earliest feature might be produced by an additional physical ingredient, such as an abrupt energy injection, before the forward-shock emission from the off-axis jet. Thus, this model is also possible.

*Dust scattering model.* The dust scattering model was proposed to explain the shallow-decay phase of *Swift* GRBs (Shao & Dai 2007), as in the optically dark GRB 090417B (Holland et al. 2010). However, one prediction of this model is that the spectral index would be softer by about  $\Delta\beta = 2-3$  in the dust scattering procedure (Shen et al. 2009) across the break from the shallow-decay segment to the normal-decay phase. This prediction is not consistent with the case of GRB 090529A. Thus, this model can be excluded.

*Photosphere + external-shock model.* Wu & Zhang (2011) have recently proposed that the X-ray afterglow is dominated by the photospheric emission of a long-lasting wind, while the optical afterglow is dominated by synchrotron emission of the forward shock. Within this model, if the long-lasting central engine has a break in the luminosity time history (e.g. Dai & Lu 1998b; Zhang &

Mészáros 2001), both the X-ray and optical light curves can show an achromatic break at the time of the central engine break, if the total energy injected from the long-lasting engine exceeds that in the blast wave at early times. This model could interpret the data of GRB 090529A, but it requires that the optical and X-ray emissions of this burst should be dominated by totally different processes.

Moreover, the optical and X-ray emissions during the shallow-decay phase have different temporal indices, which could be a result of the emissions of the forward and reverse shocks of a relativistic wind bubble around the central engine (Dai 2004). Recently, Shen & Matzner (2012) have proposed a new model to interpret the shallow-decay phase in the GRB afterglows, as for GRB 090529A. This model does not require energy injection, but attributes the shallow decay to the coasting phase of the blast wave in wind medium, while the subsequent normal decay is from the standard decelerating phase of the blast wave in the same type of medium.

## 4 ENERGY BUDGET

GRBs are believed to be produced by ultrarelativistic outflows that are collimated into narrow jets (e.g. see the review by Granot & Ramirez-Ruiz 2010). A break in the multiwavelength light curves is expected when the Lorentz factor  $\gamma$  drops below the inverse of the angular width of the jet  $\theta$  (Rhoads 1999; Sari, Piran & Halpern 1999). For GRB 090529A, this type of jet break is not observed, as shown in Fig. 1, which indicates that the time of a possible jet break should be later than the last observation of the X-ray afterglow,  $t_{\text{jet,s}} > 10^6$  s. Following Sari et al. (1999), the jet half-opening angle  $\theta$  for an ISM environment can be estimated as  $\theta = 0.161 \times (t_{\text{jet,d}}/(1+z))^{3/8} \times (n \times \eta_\gamma/E_{\gamma,\text{iso},52})^{1/8}$ , where  $z$  is the redshift and  $t_{\text{jet,d}}$  is the break time in days. Here,  $\theta$  is not sensitive to the isotropic energy  $E_{\text{iso}}$ . Assuming typical values of  $n = 0.1 \text{ cm}^{-3}$  and  $\eta_\gamma = 0.2$  (Gao & Dai 2010), the opening angle of the jet  $\theta$  should be larger than  $6.84^\circ$ . This half-opening angle is larger than those of most GRBs (Gao & Dai 2010). With the relation of  $E_\gamma = (1 - \cos\theta)E_{\gamma,\text{iso}}$ ,  $E_\gamma$  is estimated to be about  $5 \times 10^{50}$  erg.

## 5 SUMMARY AND CONCLUSION

We have reported on optical observations of GRB 090529A from various ground-based telescopes. The optical light curve shows a shallow-decay phase from  $\sim 2000$  s after the burst with a decay index of about 0.37. This is followed by a ‘normal’ decay segment starting at about  $10^5$  s after the burst. Before the shallow-decay phase in the optical afterglow, a tentative flare-like event or re-brightening exists at earlier times ( $< 2000$  s), according to the observations of the UVOT. Meanwhile, the X-ray afterglow shows a canonical light curve. The shallow-decay phase in the X-ray afterglow starts at about 3000 s after the burst, and ends at  $\sim 10^5$  s, showing a decay index of about 0.04. The later phase after the break ( $> 10^5$  s) in both the X-ray and optical afterglows can be explained using the standard forward-shock model without any energy injection in the case of  $\nu_x > \max(\nu_c, \nu_m)$  in an ISM. During our observations, no jet break signature is detected. The time for jet break should be later than the end time of the X-ray observations ( $\sim 10^6$  s), which indicates that the half-opening angle of the jet is larger than  $6.84^\circ$  and that the collimated-corrected energy is about  $5 \times 10^{50}$  erg. This means that this burst is consistent with the Ghirlanda relation.

To model the simultaneous shallow-decay phase in both the X-ray and optical afterglows, an energy injection into a wind-type medium is needed. However, there is also a constraint of the spectral condition of  $\nu_m < \nu_o < \nu_x < \nu_c$ , which is not consistent with the

observations of optical multiband observations. Moreover, the transition break between the shallow-decay and normal-decay phases is not only a result of the cessation of energy injection, but it also corresponds to the transition of the external medium density from a wind-type medium to an ISM. However, it is unlikely that these two different processes take place at the same time. Other models, such as evolving microphysical parameters and the off-axis viewing jet model, are also possible for the shallow-decay phase.

## ACKNOWLEDGMENTS

We thank the anonymous referee for comments that have helped us to improve the paper. We also wish to thank Bing Zhang for useful discussions on the modelling of this burst. This work made use of data supplied by the UK *Swift* Science Data Centre at the University of Leicester. This work is supported by the Young Researcher Grant of National Astronomical Observatories, Chinese Academy of Sciences. LPX acknowledges the support of the National Natural Science Foundation of China (NSFC) grant 11103036. CW acknowledges the support of the NSFC grant 10903010. DAK thanks U. Laux for help with obtaining the observations and B. Stecklum for observing time. AP and AV acknowledge the support of Russian Foundation for Basic Research (RFFI) grants 10-07-00342\_a and 11-01-92202Mong\_a. JPUF acknowledges the support of the European Research Council Starting Grant EGG-278202. GL is supported by the Carlsberg Foundation. The Dark Cosmology Centre is funded by the Danish National Research Foundation. This work is partly based on observations made with the NOT, operated on the island of La Palma jointly by Denmark, Finland, Iceland, Norway and Sweden, in the Spanish Observatorio del Roque de los Muchachos of the Instituto de Astrofísica de Canarias.

## REFERENCES

- Adelman-McCarthy J. K. et al., 2008, *ApJS*, 175, 297  
Akerlof C. et al., 1999, *Nat*, 398, 400  
Amati L. et al., 2002, *A&A*, 390, 81  
Balman S. et al., 2009, *GCN Circ.*, 9485, 1  
Cenko S. B. et al., 2011, *ApJ*, 732, 29  
Chevalier R. A., Li Z.-Y., 1999, *ApJ*, 520, L29  
Chevalier R. A., Li Z.-Y., 2000, *ApJ*, 536, 195  
Covino S. et al., 2008, *MNRAS*, 388, 347  
Curran P. A., Evans P. A., de Pasquale M., Page M. J., van der Horst A. J., 2010, *ApJ*, 716, L135  
Dai Z. G., 2004, *ApJ*, 606, 1000  
Dai Z. G., Cheng K. S., 2001, *ApJ*, 558, L109  
Dai Z. G., Lu T., 1998a, *MNRAS*, 298, 87  
Dai Z. G., Lu T., 1998b, *A&A*, 333, L87  
Dai Z. G., Lu T., 1998c, *Phys. Rev. Lett.*, 81, 4301  
Dai Z. G., Lu T., 2002, *ApJ*, 565, L87  
Dai Z. G., Wu X. F., 2003, *ApJ*, 591, L21  
Dai X., Halpern J. P., Morgan N. D., Armstrong E., Mirabal N., Haislip J. B., Reichart D. E., Stanek K. Z., 2007, *ApJ*, 658, 509  
de Ugarte Postigo A. et al., 2005, *A&A*, 443, 841  
de Ugarte Postigo A. et al., 2007, *A&A*, 462, L57  
Eichler D., Granot J., 2006, *ApJ*, 641, L5  
Evans P. A. et al., 2009, *MNRAS*, 397, 1177  
Gao Y., Dai Z.-G., 2010, *Res. Astron. Astrophys.*, 10, 142  
Gehrels N. et al., 2004, *ApJ*, 611, 1005  
Granot J., 2006, *Nuovo Cim. B*, 121, 1073  
Granot J., Ramirez-Ruiz E., 2010, in Kouveliotou C., Woosley S. E., Wijers R. A. M. J., eds, *Gamma-Ray Bursts*. Cambridge Univ. Press, Cambridge, in press (arXiv:1012.5101)  
Granot J., Panaitescu A., Kumar P., Woosley S. E., 2002, *ApJ*, 570, L61  
Granot J., Königl A., Piran T., 2006, *MNRAS*, 370, 1946  
Grupe D. et al., 2007, *ApJ*, 662, 443  
Holland S. T. et al., 2010, *ApJ*, 717, 223  
Kouveliotou C., Meegan C. A., Fishman G. J., Bhat N. P., Briggs M. S., Koshut T. M., Paciesas W. S., Pendleton G. N., 1993, *ApJ*, 413, L101  
Liang E.-W., Zhang B.-B., Zhang B., 2007, *ApJ*, 670, 565  
Liang E.-W., Racusin J. L., Zhang B., Zhang B.-B., Burrows D. N., 2008, *ApJ*, 675, 528  
Liang E.-W., Yi S.-X., Zhang J., Lü H.-J., Zhang B.-B., Zhang B., 2010, *ApJ*, 725, 2209  
Lipkin Y. M. et al., 2004, *ApJ*, 606, 381  
Lupton R. H. et al., 2005, *AAS Meeting 207*, 133.08; *Bull. Am. Astron. Soc.*, 37, 1384  
Malesani D., Fynbo J. P. U., D’Elia V., de Ugarte Postigo A., Jakobsson P., Thöne C. C., 2009, *GCN Circ.*, 9457, 1  
Markwardt C. B. et al., 2009, *GCN Circ.*, 9434, 1  
Marshall F. E. et al., 2011, *ApJ*, 727, 132  
Mészáros P., Rees M. J., Wijers R. A. M. J., 1998, *ApJ*, 499, 301  
Monfardini A. et al., 2006, *ApJ*, 648, 1125  
Nousek J. A. et al., 2006, *ApJ*, 642, 389  
Paczynski B., 1998, in Meegan C. A., Koshut T. M., Preece R. D., eds, *AIP Conf. Ser. Vol. 428, Fourth Huntsville Gamma-Ray Burst Symposium*. Am. Inst. Phys., New York, p. 783  
Page K. L. et al., 2007, *ApJ*, 663, 1125  
Panaitescu A., Mészáros P., Burrows D., Nousek J., Gehrels N., O’Brien P., Willingale R., 2006, *MNRAS*, 369, 2059  
Rau A. et al., 2010, *ApJ*, 720, 862  
Rhoads J. E., 1999, *ApJ*, 525, 737  
Sakamoto T. et al., 2009a, *GCN Circ.*, 9430, 1  
Sakamoto T., Krimm H. A., Sbaruffati B., Schady P., 2009b, *GCN Rep.*, 225, 1  
Sakamoto T. et al., 2009c, *ApJ*, 692, 922  
Sari R., Mészáros P., 2000, *ApJ*, 535, L33  
Sari R., Piran T., Narayan R., 1998, *ApJ*, 497, L17  
Sari R., Piran T., Halpern J. P., 1999, *ApJ*, 519, L17  
Schlegel D. J., Finkbeiner D. P., Davis M., 1998, *ApJ*, 500, 525  
Shao L., Dai Z. G., 2007, *ApJ*, 660, 1319  
Shen R., Matzner C. D., 2012, *ApJ*, 744, 36  
Shen R.-F., Willingale R., Kumar P., O’Brien P. T., Evans P. A., 2009, *MNRAS*, 393, 598  
Thöne C. C. et al., 2010, *A&A*, 523, A70  
Updike A. C. et al., 2008, *ApJ*, 685, 361  
Urata Y. et al., 2007, *ApJ*, 668, L95  
Volnova A., Naumov K., Kouprianov V., Devyatkin A., Pozanenko A., 2009, *GCN Circ.*, 9611, 1  
Woźniak P. R., Vestrand W. T., Wren J. A., White R. R., Evans S. M., Caspersen D., 2006, *ApJ*, 642, L99  
Wu X. F., Zhang B., 2011, *ApJ*, submitted  
Xin L. P. et al., 2010, *MNRAS*, 401, 2005  
Yamazaki R., 2009, *ApJ*, 690, L118  
Zhang B., Mészáros P., 2001, *ApJ*, 552, L35  
Zhang B., Fan Y. Z., Dyks J., Kobayashi S., Mészáros P., Burrows D. N., Nousek J. A., Gehrels N., 2006, *ApJ*, 642, 354  
Zhang B. et al., 2009, *ApJ*, 703, 1696

This paper has been typeset from a  $\text{\TeX}/\text{\LaTeX}$  file prepared by the author.